Turkish Journal of Physics

http://journals.tubitak.gov.tr/physics/

Research Article

Turk J Phys
(2019) 43: 196 – 206

doi:10.3906/fiz-1812-2

# The influence of crosslinking temperature on the spectroscopic, thermal, and mechanical properties of poly(vinyl alcohol)/zeolite composites

**Cenk DENKTAŞ***
Department of Physics, Faculty of Science, Yıldız Technical University, İstanbul, Turkey

**Received:** 04.12.2018 • **Accepted/Published Online:** 18.03.2019 • **Final Version:** 08.04.2019

**Abstract:** The aim of this study was to understand the effect of crosslinking temperature on the spectroscopic, thermal, and mechanical properties of poly(vinyl alcohol) (PVA)/zeolite composites. The PVA nanocomposite films were prepared using the solvent casting method with tartaric acid as the crosslinker. The changes in the structures of pure PVA film and powder clinoptilolite (CL) and nanocomposite films were analyzed by means of ATR-FTIR spectroscopy. The effect of both crosslinking temperature and CL on the composite films prepared by the addition of constant CL to the polymer matrix at different crosslinking temperatures (series II) and pure PVA films prepared with different crosslinking temperatures (series III films) shows that the tensile strengths increase with increasing crosslinking temperature, while the elongation at break of films decreases due to the crosslinking temperature and CL. The differential scanning calorimetry results show that the crosslinking temperature leads to an increase in the glass transition ($T_g$) of nanocomposites. According to the results of this study, both zeolite and crosslinking temperature affect the thermal and mechanical properties of the material. These results may be used for membrane technology.

**Key words:** Poly(vinyl alcohol), crosslinking temperature, differential scanning calorimetry, mechanical properties, microstructure

## 1. Introduction

Poly(vinyl alcohol) (PVA) is a typical hydrophilic and hydroxyl-rich polymer obtained by polymerization of vinyl alcohol. PVA has good film-forming properties, mechanical properties, nontoxicity, biocompatibility, and chemical stability due to the abundance of hydroxyl groups [1]. It has vast areas of application such as excellent membrane materials [2], medical materials [3], and food packaging materials [4].

In recent years, zeolites have gained attention due to their high melting points (above 1000 °C) and high resistance under pressure. In addition, they do not dissolve in water or inorganic solvents and do not undergo oxidation in air. Zeolites are represented by the following formula:

$$M_{2/n}O \cdot Al_2O_3 \cdot {}_xSiO_2 \cdot {}_y H_2O_2 \cdot 0,$$

where (x) and (y) are the stoichiometric coefficients of the $Si^{4+}$ and $Al^{3+}$ in the tetrahedra and M is the exchangeable cation of valence n [5]. There are different types of zeolite minerals: natural (clinoptilolite (CL), chabazite, and modernite) and synthetic zeolites (zeolite A; zeolites X and Y) [6]. Among them, CL, which is the member of the heulandite (HEU) family of zeolites having a Si/Al ratio greater than 4, is the most common

*Correspondence: cdenktas@yildiz.edu.tr

and abundant natural zeolite in the world. It possesses plates or laths with tabular form structure [7]. Moreover, total zeolite reserves are estimated to be around 50 billion tons in Turkey [8].

As PVA is soluble in water due to its high hydrophilic nature, its application areas are limited [9,10]. For this reason, crosslinking agent and different nanosized fillers (sodium montmorillonite, zeolite 4A, NaX, NaY, silicalite-1, and ZSM-5 zeolite) are used to improve the water resistance and separation efficiency of PVA, respectively [11–18]. Furthermore, the crosslinking agent and crosslinking temperature are known to have a significant effect on the hydrophilic structure of polymers [18,19]. Recent studies have shown a strong relation between heat treatment and the crosslinking agent [9,20]. Research on the crosslinking agent is broad [21,22], but there is little research on both crosslinking temperature [23,24] and zeolite [13,25] on PVA at the same time. In a previous study, the optimum temperature and time for crosslinking of PVA with the maleic acid agent were found [26]. Studies in the literature relate to crosslinking temperature and its effect on the PDMS polymer [27,28]. There is no report regarding the effect of crosslinking temperatures on the microstructure or mechanical or thermal properties of PVA/CL composite.

The main aim of the present study was to investigate the effect of different crosslinking temperatures (100, 120, and 140 °C) on PVA/zeolite composites. The composites were characterized for microstructure composition using Fourier transform infrared (FTIR)/attenuated total reflectance (ATR) spectroscopy and field emission scanning electron microscope (FE-SEM) and EDX analysis. Mechanical tests were carried out on a Lloyd tensile testing machine, while thermal properties were determined by differential scanning calorimetry (DSC).

## 2. Experimental

### 2.1. Materials and sample preparation

The PVA and CL ($(Na_{0.5}K_{2.5})\ (Ca_{1.0}Mg_{0.5})(Al_6Si_{30})O_{72}.24H_2O$, Gördes, Turkey) were supplied by Sigma-Aldrich and Incal Mineral Co, respectively. Samples were prepared in two different stages. In the first step, zeolite was added to the polymer matrix and crosslinking temperature was applied. In the second step, the crosslinking temperature was also applied to pure PVA film without the addition of zeolite. PVA was dissolved in distilled water at low mixing speed at 90 °C for 3 h in order to produce a 15 wt.% solution. The amount (5 wt.%) of constant CL was incorporated into the solution during the preparation of the PVA solution. The tartaric acid (TA) solution of 15?wt % was prepared by mixing for 1 h at room temperature. The calculated amounts of the two solutions [(PVA + CL) + TA] were mixed together at room temperature for 1?h. The prepared solution was cast onto Plexiglas plates as thin films to dry at 50 °C in the oven for a day. Then the composites were crosslinked at different temperatures (100, 120, and 140 °C) in the oven for 45 min. All samples were kept in pure water for the removal of unreacted crosslinker, monomer, and impurities at room temperature overnight. After that the membranes were dried at 105 °C for 2?h. The thicknesses of all the samples measured were in the range of 100–292?µm. Three different serial samples were prepared for investigation: (1) Series 1, pure PVA film, powder CL, and pure PVA + CL (PC) film are shown. (2) Series 2, samples 4–6 belonging to composite films prepared by the addition of the constant CL to the polymer matrix at different crosslinking temperatures (100, 120, and 140 °C) are shown. (3) Series 3 (samples 7–9) shows pure PVA films prepared with different crosslinking temperatures (100, 120, and 140 °C).

### 2.2. FTIR/ATR spectroscopic method

The structural changes in samples were recorded by an Agilent Technologies Cary 630 FTIR apparatus at room temperature. Spectra of all samples were recorded in the 600–4000?cm$^{-1}$ range at a resolution of 4?cm$^{-1}$ with 32 scans for each measurement.

### 2.3. FE-SEM and EDX analysis

The surface and cross-sectional morphology of the powder CL, pure PVA film, and PC film was observed by FE-SEM (FEI Quanta 450 scanning electron microscope (SEM)), with an accelerating voltage of 15 kV and high pressure. The powder CL, pure PVA film, and PC film were examined by X-ray spectroscopy (EDX); the operating voltage used was 30 kV.

### 2.4. Tensile testing measurements

The stress-strain curves of sample films were determined by a Lloyd tensile testing machine (AMETEK, Lloyd Instruments, Bognor Regis, UK) with a crosshead speed of 10 mm/min at 20 °C and a relative humidity of 65%. The films had dimensions of length 25 mm × width 6 mm. The average value of the six experimental samples was analyzed.

### 2.5. Thermal analysis

The DSC measurements of the PVA/clino membranes were carried out using a PerkinElmer DSC-7. Pieces cut from the polymer film to a mass of approximately 5 mg for DSC measurements were loaded into aluminum pans and crimped. Temperature ranges were selected between 30 °C and 300 °C with a heating rate of 10 °C/min for DSC measurements. The DSC instrument was calibrated with the standard indium. The glass transition ($T_g$) and the melting temperature ($T_m$) were determined from the second scan curves of DSC.

## 3. Results

### 3.1. FTIR/ATR spectral analysis

The microstructural changes in all samples were examined with the FTIR spectroscopic method and are given in Figure 1. For the pure PVA film, the strong and broad band at 3690–2996 cm$^{-1}$ was related to the O–H stretching frequencies of PVA's wide distribution of hydrogen bonding among the hydroxyl groups from molecular water (Figure 1a). As shown in Figure 1b, changes in the intensity and position of this peak for samples 4–6 were representative of the interactions between the PVA and CL after treatment at different crosslinking temperatures [29,30]. After modification of zeolite with PVA at 140 °C, the OH stretching frequency of the PVA shifted from 3309 to 3250 cm$^{-1}$, which indicates the formation of crosslinking between PVA, TA, and CL to form a solid compound through the hydrogen bonding mechanism [31–34]. The specific peaks at 2922 cm$^{-1}$ and 1319 cm$^{-1}$ were related to the presence of the C–H stretching and bending of PVA chains, respectively. In the wavenumber range 782 cm$^{-1}$ corresponds to the allotropic phase of $SiO_2$ or the Si–O bonds, which are the result of the $SiO_4$ tetrahedral in the CL framework [35–37]. The vibrational small peak at 834 cm$^{-1}$ is attributed to the C–H rocking of pure PVA [38]. It can be seen from Figure 1a that the sharp peak around 1021 cm$^{-1}$ region was related to internal bonding in the CL framework and Si–O stretching [30,36]. The peaks at 1640 cm$^{-1}$ and 1528 cm$^{-1}$ are assigned to the presence of bending vibration of molecular water in the CL

framework and vibration of the bond Si–O [36,37,39]. The two small peaks at 3615 $cm^{-1}$ and 3734 $cm^{-1}$ are associated with two different Brønsted sites and as well as 3678 $cm^{-1}$ (Si–OH) and 3743 $cm^{-1}$ (Al–OH) [19]. As shown in Figure 1c, the specific peaks of series 3 do not show any significant change after the treatment at different crosslinking temperatures. However, after treatment with crosslinking temperature and zeolite effect, there was a change in the intensity of the films in series 2. This result can be said to be due to the CL filler having a greater effect than the crosslinking temperature on the polymer matrix.

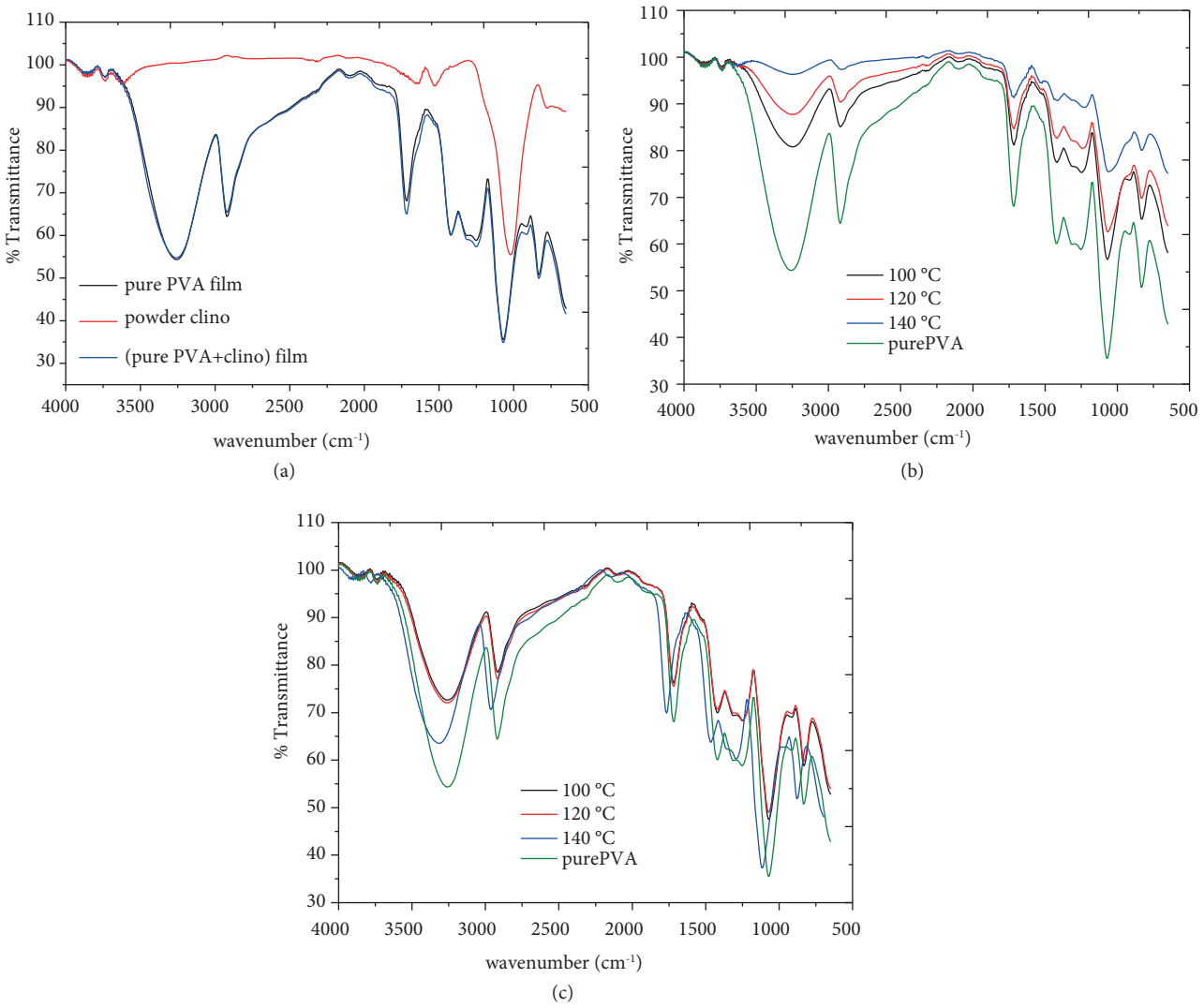


**Figure 1**. FTIR spectra of (a) samples 1–3 (samples series 1, pure PVA film, PC film), (b) 4–6 (series 2), and (c) 7–9 (series 3).

### 3.2. Morphological analysis

The surface and cross-sectional morphology of the pure PVA film, PC film, and powder CL was observed by FE-SEM (Figure 2). As seen from Figure 2a, the zeolite particles have an average grain size of about 15–50 µm. The SEM images taken from the cross-sections of the pure PVA shown in Figure 2b did not show zeolite particles.

When tartaric acid enters the polymer matrix as a crosslinking agent, it exhibits a crystalline structure in the structure formed (Figure 2c). TA is known to have a crystalline structure [40,41]. However, no effect of TA on the surface morphology of PVA polymer matrix composites has been reported in the literature. The FE-SEM surface and cross-section micrographs of the pure PVA + CL (PC) film indicate that the zeolite particles are uniformly distributed on the PVA matrix (Figures 2d and 2e) and no aggregation of zeolite particles is observed. These results suggested that when the value of $T_g$ increases with the introduction of zeolite into a polymer matrix, it can be concluded that the interaction between the polymer matrix and zeolite did indeed take place. EDX mapping was performed to confirm the homogeneous distribution of zeolite in the membrane and zeolite was found to contain aluminum and silicon. Figure 3 shows the SEM of a typical portion of the surface of the powder CL particles and the PC film for receiving the EDX map of the same area. The zeolite appears to contain silicon, aluminum, potassium, and calcium. Then the image revealed that the silicon distribution was the same across the surface of the sample.

### 3.3. Mechanical properties

The curves of stress ($\sigma$, MPa) versus strain (% $\varepsilon$) during the tension of the pure PVA film, PPC, series 2, and series 3 are given in Figure 4 at room temperature. The results for mechanical properties obtained from the stress-strain curves are given in Table 1. The tensile strength, elongation at break, and work to break for pure PVA film are 52.141 MPa, 323.66%, and 1576.67 Nmm, respectively (Figure 4). As shown in Table 1, there is a statistically significant difference between the pure PVA film and series 2 and series 3.

**Table 1**. Mechanical test results of pure PVA film, P + PC film, samples 4–6 (series 2), and samples 7–9 (series 3).

| Samples | | Tensile stress at break (MPa) | Elongation at break (mm/mm) | Work to break (N mm) |
|---|---|---|---|---|
| Pure PVA | | 52.141 | 323.66 | 1576.67 |
| PC | | 49.415 | 300.66 | 1333.30 |
| Series 2 | 100 °C | 56.984 | 239.36 | 917.75 |
| | 120 °C | 51.115 | 186.33 | 877.25 |
| | 140 °C | 63.374 | 100.09 | 546.73 |
| Series 3 | 100 °C | 43.751 | 233.49 | 1192.13 |
| | 120 °C | 37.831 | 103.96 | 480.51 |
| | 140 °C | 45.693 | 32.84 | 172.15 |

As seen from Table 2, since the glass transition ($T_g$) of pure PVA is higher than room temperature, it has more amorphous phase [42]. The tensile strength of series 2 increased with the increase in crosslinking temperatures except for pure PVA membrane (in Table 1). It is thought that zeolite particles in the polymer matrix can behave as physical crosslinkers or the intermolecular interactions between polymer matrix and zeolite lead to stronger film structure and improved mechanical properties [43–45]. When we compare series 3 with pure PVA, it is seen from Figure 4b that the shape of the stress-strain curve changed at crosslinking temperatures above $T_g$. It is known that PVA is a semicrystalline polymer and the reduction in tensile strength with increasing temperature was noticeably small [42,46].

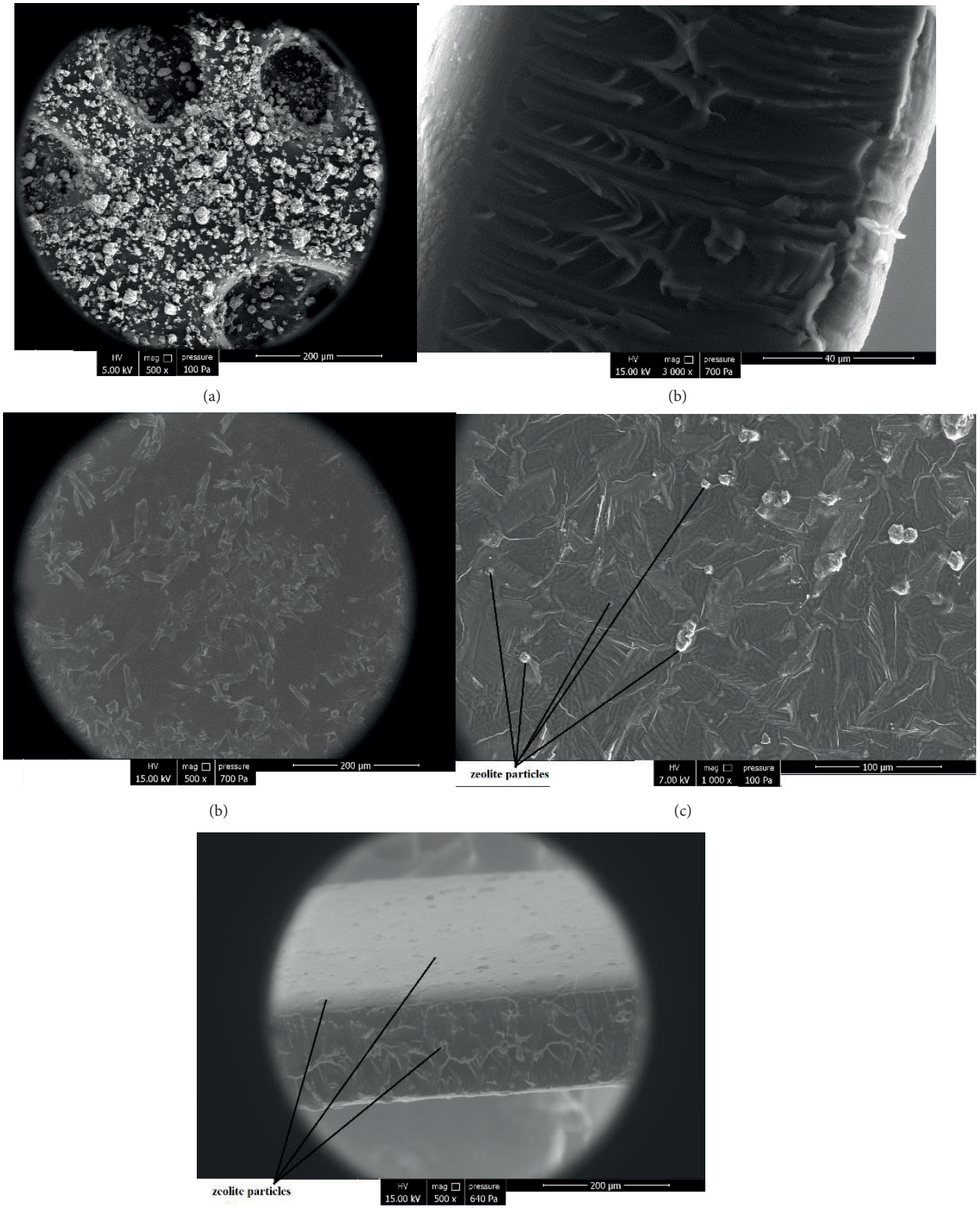


**Figure 2**. FE-SEM of a randomly selected area on the (a) powder CL particles, (b) cross-section of pure PVA film, (c) surface of pure PVA film, (d) surface of pure PC film, and (e) surface and cross-section of PC film.

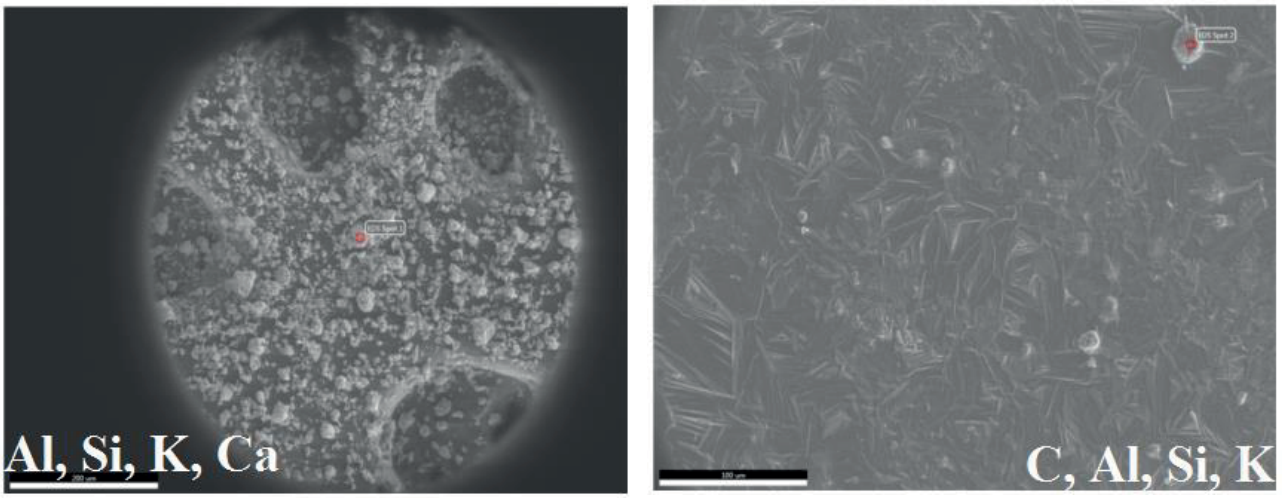


(a) (b)

**Figure 3**. EDX analysis of (a) powder CL and (b) PC film.

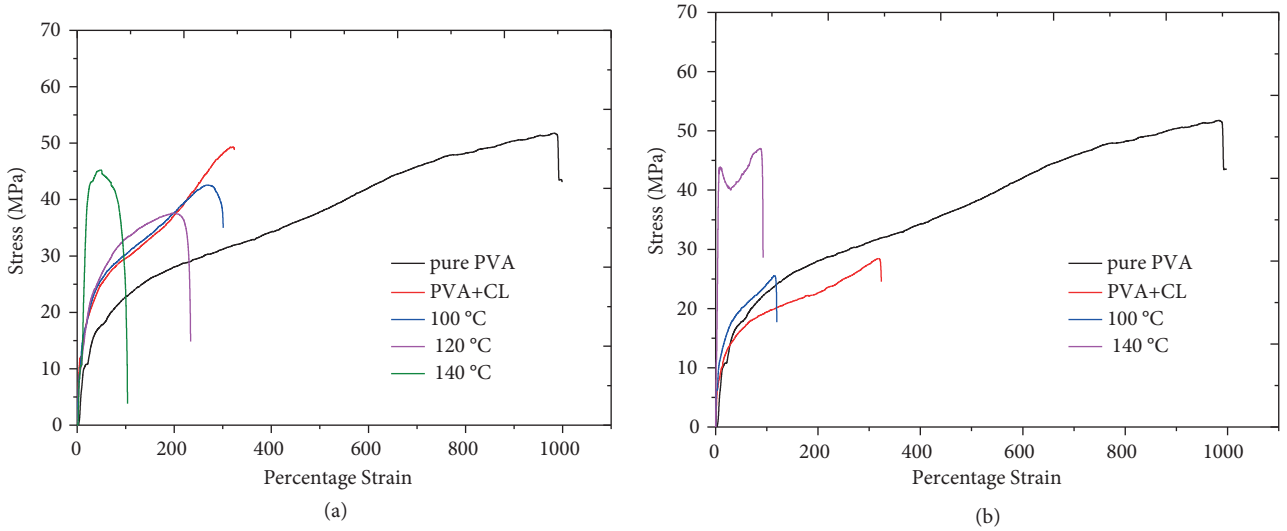


**Figure 4**. The stress-strain curves for samples: (a) pure PVA film, PC film, and series 2 and (b) pure PVA film and series 3.

As shown in Table 1, the elongation at break of series 2 and series 3 samples decreased significantly with increasing crosslinking temperature, while in the PC film it remained almost unchanged. This result indicates that series 2 and series 3 films became somewhat more brittle compared to the pure PVA film. However, the PC film exhibits elastic behavior.

For all samples, work to break, which is the required energy per volume to break, was determined from the area under the stress-strain trace and the results are given in Table 1. The work to break of series 2 and series 3 samples decreased with increasing crosslinking temperature, which may be ascribed to the increased frequency of localized clusters or aggregations [47]. For instance, the work to break of the series 3 sample was approximately 1/3 of that of the series 2 sample at 140 °C.

**Table 2**. Thermal properties from DSC of pure PVA film, PC film, series 2, and series 3.

| Sample | | $T_g$ (°C) | $T_m$ (°C) |
|---|---|---|---|
| Pure PVA film | | 63.55 | 234.90 |
| PC film | | 147.03 | 234.39 |
| Series 2 | 100 (°C) | 146.78 | 234.54 |
| | 120 (°C) | 146.22 | 234.53 |
| | 140 (°C) | 147.10 | 234.35 |
| Series 3 | 100 (°C) | 141.99 | 235.03 |
| | 120 (°C) | 137.03 | 234.48 |
| | 140 (°C) | 140.84 | 234.36 |

### 3.4. Thermal properties of composite films

The thermal properties of the samples were investigated using DSC. Figure 5 illustrates the DSC thermograms during the second heating for all samples and the onset, $T_m$ and $T_g$, given in Table 2.

The pure PVA film (Figure 5a) has an endothermic reaction at 63.55 °C, which is attributed to the glass transition temperature ($T_g$) [48]. When compared to the pure PVA, studies show a noticeable increase in $T_g$ of the samples (series 2 and series 3) based on crosslinking temperature as shown in Table 2. This result indicates that the segmental motion of the polymer chains due to both addition of the CL filler and the crosslinking effect on the polymer matrix is prevented [49,50]. Then $T_g$ of the series 2 samples shifted to higher temperatures due to the effect of the CL filler in the PVA matrix (Table 2). From Figure 5a it can be seen that the small endothermic peak at 234.90 °C (the first peak) for pure PVA film was related to the crystalline phases of PVA [51–53]. However, the DSC thermograms show that the second melting peak is virtually unchanged with both CL and rising crosslinking temperatures. This result shows also that the crosslinking and CL filler affected the amorphous region of the PVA matrix [54].

## 4. Conclusions

In this work, PVA/zeolite composites were successfully prepared. The pure PVA membrane and PVA/zeolite composites were crosslinked at different temperatures (100, 120, and 140 °C). The morphologies and microstructures of the PVA/zeolite composites were characterized and assessed using FE-SEM and EDX, ATR-FTIR spectral analysis, and thermal characteristic (DSC) and mechanical properties.

1. FTIR/ATR spectral results indicate that the CL filler has a greater effect than the crosslinking temperature on the polymer matrix.

2. As seen from Table 2, since the glass transition ($T_g$) of pure PVA is higher than room temperature, it has more amorphous phase. This shows that pure PVA membrane has higher extensibility than series 2 and series 3, whereas in series 2 it causes a stronger and harder film structure due to intermolecular interactions between the polymer matrix and zeolite particles [42]. It is clearly shown that pure PVA is a mechanical sensitive material due to varying crosslinking temperature [55]. The effect of crosslinking temperature on the mechanical properties of PVA is remarkable at 100 °C. Crosslinking is observed as the elongation of the material decreases.

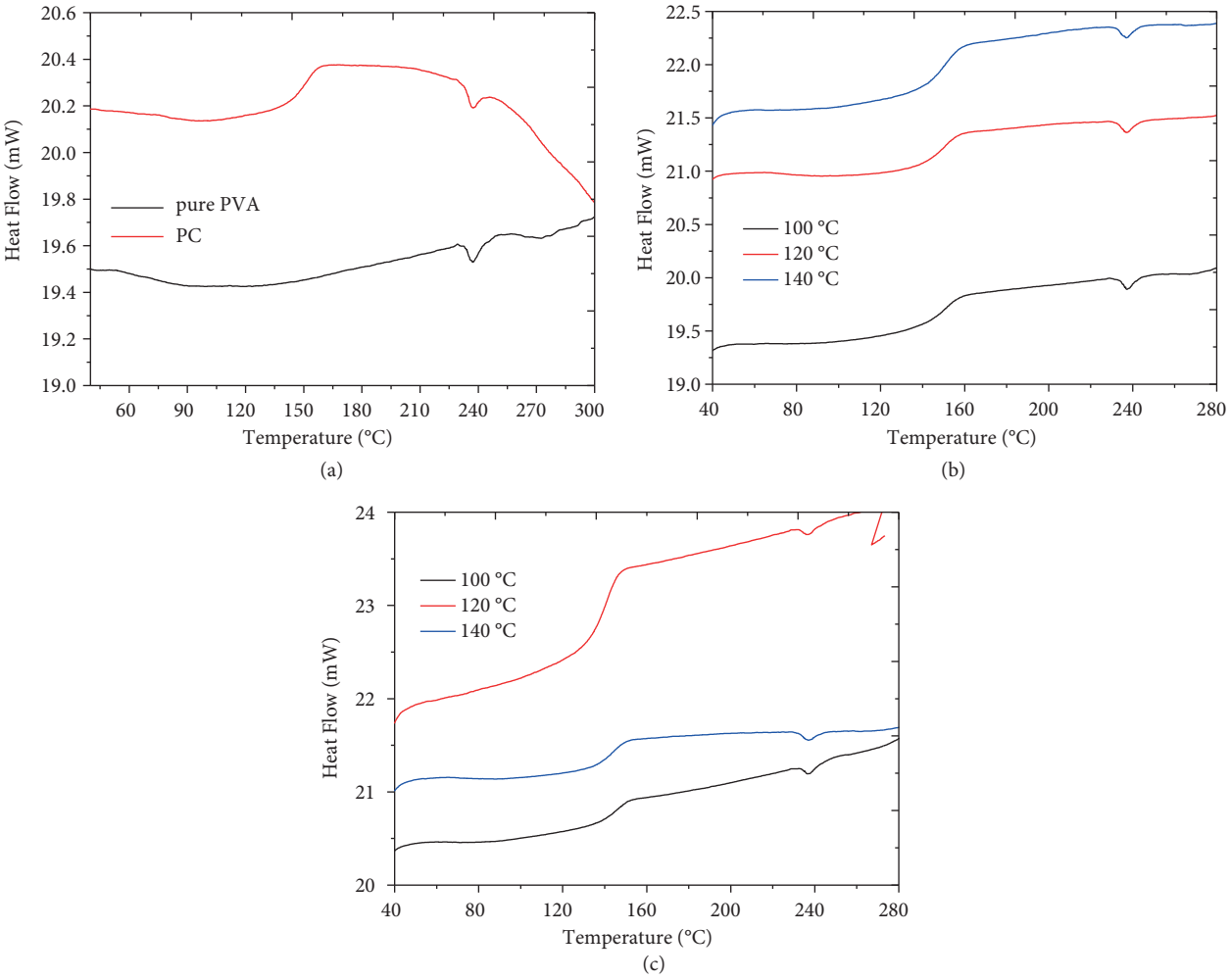


**Figure 5**. DSC thermograms of (a) pure PVA film and PC film, (b) samples 4–6 (series 2), and (c) samples 7–9 (series 3).

3. As a result of DSC analyses, a significant increase of approximately 200% was observed in the $T_g$ of P + PC film, series 2, and series 3 samples, while the melting temperature ($T_m$) remained almost unchanged. From the results in Table 2, when compared to the pure polymer, the increase in the glass transition temperature for crosslinking temperature and PVA treated with zeolite indicates no effect on the crystalline regions of the polymer.

4. In general, this study is part of an ongoing study, and in future research the sorption properties for the ethanol/water mixture using PVA doped with different zeolites will be studied.

## References

[1] Choo, K.; Ching, Y. C.; Chuah, C. H.; Julai, S.; Liou, N. S. *Materials* **2009**, *6*, 644.

[2] Finch, C. A. *Polyvinyl Alcohol: Properties and Applications*; Wiley: New York, NY, USA, 1973, pp. 105-106.

[3] Paradossi, G.; Cavalieri, F.; Chiessi. *E. J. Mater. Sci.-Mater. M.* **2003**, *14*, 687-691.

[4] Demerlis, C. C.; Schoneker, D. R. *Food Chem. Toxicol.* **2003**, *41*, 319-326.

[5] Breck, D. W. *Zeolite Molecular Sieves, Structure Chemistry and Use*; Wiley: New York, NY, USA, 1974.

[6] Zamzow, M. J.; Eichbaum, B. R.; Sandgren, K. R.; Shanks, D. E. *Sep. Sci. Technol.* **1990**, *25*, 1555-1569.

[7] Moraetis, D.; Christidis, G. E.; Perdikatsis, V. *Am. Mineral.* **2007**, *92*, 1714-1730.

[8] Devlet Planlama Teşkilatı(DPT). *Madencilik Özel İhtisas Komisyonu Endüstriyel Hammaddeler Alt Komisyonu-Diğer Endüstri Mineralleri Çalışma Grubu Raporu*; DPT: Ankara, Turkey, 1996 http://ekutup.dpt.gov.tr/madencil/sanayiha/oik480c1.pdf (in Turkish).

[9] Ding, B.; Kim, H. Y.; Lee, S. C.; Shao, C. L.; Lee, D. R., Park, S. J.; Kwag, G. B.; Choi, K. J. *J. Polym. Sci. Pol. Phys.* **2002**, *40*, 1261-1268.

[10] Hodge, R. M. *Polymer* **1996**, *37*, 1371-1376.

[11] Kuila, S. B.; Ray, S. K. *Carbohydr. Polym.* **2014**, *101*, 1154-1165.

[12] Huang, Z.; Guan, H.; Tan, W. L.; Qiao, X. Y.; Kulprathipanja, S. *J. Membr. Sci.* **2006**, *276*, 260-271.

[13] Kittur, A. A.; Kariduraganavar, M. Y.; Toti, U. S.; Ramesh, K.; Aminabhavi, T. M. *J. Appl. Polym. Sci.* **2003**, *90*, 2441-2448.

[14] Gohil, J. M.; Bhattacharya, A.; Ray, P. *J. Polym. Res.* **2006**, *13,* 161-169.

[15] Alemzadeh, I.; Vossoughi, M. *Chem. Eng. Process.* **2002**, *41*, 707-710.

[16] Figueiredo, C. S.; Alves, L. M.; Borges, C. P. *J. Appl. Polym. Sci.* **2009**, *111*, 3074-3080.

[17] Mittal, A.; Garg, S.; Kohli, D.; Maiti, M.; Jana, A. K.; Bajpai, S. *Carbohydr. Polym.* **2016**, *151*, 926-938.

[18] Kumeta, K.; Nagashima, I.; Matsui, S.; Mizoguchi, K. *Polym. J.* **2004**, *36*, 472-477.

[19] Yeh, G. S. Y.; Hosemann, R.; Loboda-Čačković, J.; Čačković, H. *Polymer* **1976**, *17*, 309-318.

[20] Stepto, R. F. T. *Polymer Networks. Principles of their Formation, Structure and Properties*; Wiley: Chichester, UK, 1998; pp. 72-88.

[21] Li, J.; Zhang, L.; Gu, J.; Sun, Y.; Ji, X. *J. Polym. Res.* **2015**, *5*, 19859-19864.

[22] Figueiredo, K. C. S.; Alves, T. L. M.; Borges, C. P. *J. Appl. Polym. Sci.* **2009**, *1*, 3074-3080.

[23] Kumeta, K.; Nagashima, I.; Matsui, S.; Mizoguchi, K. *Polym. J.* **2004**, *36*, 472-477.

[24] Yang, C. C.; Chiu, S. J.; Chien, W. C. *J. Power Sources* **2006**, *162*, 21-29.

[25] Wang, Y.; Han, Q.; Zhou, Q.; Du, X.; Xue, L. *RSC Adv.* **2016**, *6*, 66767-66773.

[26] Gohil, J. M.; Bhattacharya, A.; Ray, P. *J. Polym. Res.* **2006**, *13*, 161-169.

[27] Sadrzadeh, M.; Shahidi, K.; Mohammadi, T. *J. Membr. Sci.* **2009**, *342*, 327-340.

[28] Pinnau, I.; He, Z. *J. Membr. Sci.* **2004**, *244*, 227-233.

[29] Kim, H. G.; Kim, J. H. *Fibers Polym.* **2011**, *12*, 602-609.

30 Laksmono, J. A.; Pratiwi, I. M.; Sudibandriyo, M.; Haryono, A.; Saputra, A. H. *AIP Conf. Proc.* **2017**, *1904*, 020076.

[30] Yang, Y.; Liu, C.; Wu, H. *Polym. Test.* **2009**, *28*, 371-377.

[31] Sabarish, R.; Unnikrishnan, G. *Carbohydr. Polym.* **2018**, *199*, 129-140.

[32] Laksmono, J. A.; Sudibandriyo, M.; Saputra, A. H.; Haryono, A. *International Journal of Chemical Engineering* **2019**, *2019*, 6036479.

[33] Kim, H. G.; Kim, J. H. *Fiber Polym.* **2011**, *12*, 602-609.

[34] Malekpour, A.; Mostajeran, B.; Koohmareh, G. A. *Chem. Eng. Process.* **2017**, *118*, 47-53.

[35] Byrappa K.; Kumar, B. V. S. *Asian J. Chem.* **2007**, *19*, 4933-4935.

[36] Ruíz-Baltazar, A.; Esparza, R.; Gonzalez, M.; Rosas, G.; Pérez, R. *J. Nanomater.* **2015**, *2015*, 364763.

[37] Rajendran, S.; Sivakumar, M.; Subadevi, *R. Mater. Lett.* **2004**, *58*, 641-649.

[38] Madejova, J. *Vib. Spectrosc.* **2003**, *31*, 1-10.

[39] Altinisik, A.; Yurdakoc, K. *Polym. Bull.* **2014**, *71*, 759-774.

[40] Altınışık A. Synthesis, characterization and applications of pH and temperature sensitive hydrogels. PhD, Dokuz Eylül University, İzmir, Turkey, 2011.

[41] Bozdoğan, A.; Aksakal, B.; Şahintürk, U.; Yargı, Ö. *J. Mol. Struct.* **2018**, *1174*, 133-141.

[42] Zhao, X.; Zhang, Q.; Chen, D. *Macromolecules* **2010**, *43*, 2357-2363.

[43] Wang, J.; Wang, X.; Xu, C.; Zhang, M.; Shang, X. *Polym. Int.* **2011**, *60*, 816-822.

[44] Slark, A. T. *Polymer* **1997**, *38*, 4477-4483.

[45] Konidari, M. V.; Papadokostaki, K. G.; Sanopoulou, M. *J. Appl. Polym. Sci.* **2011**, *120*, 3381-3386.

[46] Chen, W.; Tao, X.; Xue, P.; Cheng. X. *Appl. Surf. Sci.* **2005**, *252*, 1404-1409.

[47] Xu, J.; Hua, Y.; Song, L.; Wang, Q.; Fan, W.; Liao, G.; Chen, Z. *Polym. Degrad. Stab.* **2001**, *73*, 29-31.

[48] Yin, Y.; Li, J.; Liu, Y.; Li, Z. *J. Appl. Polym. Sci.* **2005**, *96*, 1394-1397.

[49] Krumova, M.; López, D.; Benavente, R.; Mijangos, C.; Pereña, J. M. *Polymer* **2000**, *41*, 9265-9272.

[50] Martinelli, A.; Matic, A.; Jacobsson, P.; Börjesson, L.; Navarra, M. A.; Fernicola, A.; Panero, S.; Scrosati, B. *Solid State Ionics* **2006**, *177*, 2431-2435.

[51] Teli, S. B.; Calle, M.; Li, N. J. *Membr. Sci.* **2011**, *371*, 171-178.

[52] Jelinska, N.; Kalnins, M.; Tupureina, V.; Dzene, A. *Materials Science and Applied Chemistry* **2010**, *21*, 55-61.

[53] Morimune, S.; Nishino, T.; Goto, T. *Polym. J.* **2012**, *44*, 1056-1063.

[54] Es-Saheb, M.; Elzatahry, A. *Int. J. Polym. Sci.* **2014**, *2014*, 605938.